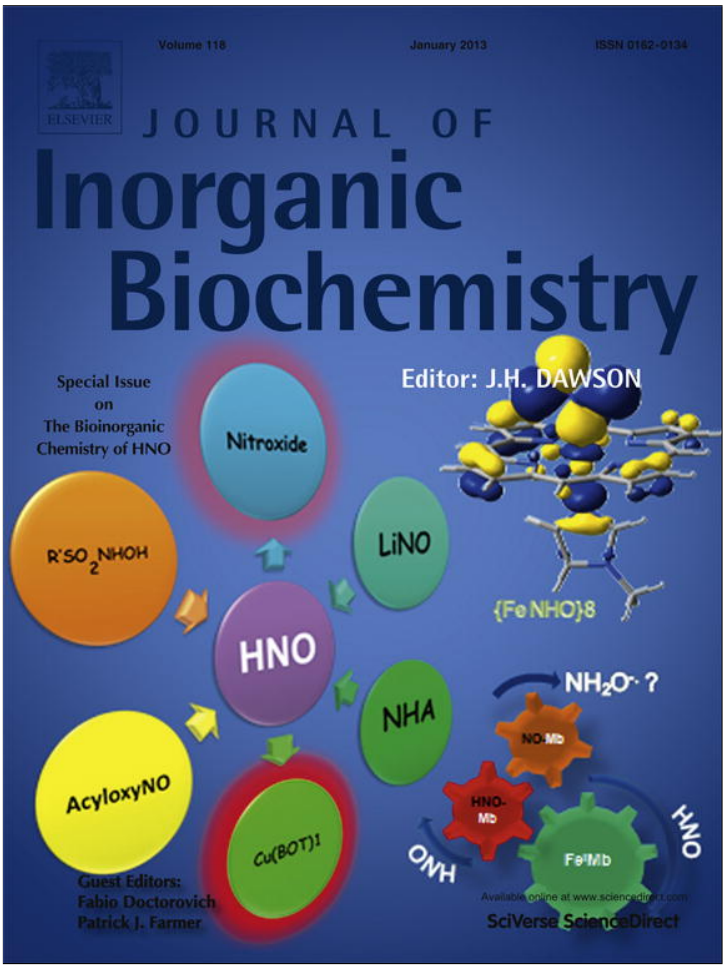

Journal of Inorganic Biochemistry 118 (2013) 134–139

Contents lists available at SciVerse ScienceDirect

Journal of Inorganic Biochemistry

journal homepage: www.elsevier.com/locate/jinorgbio

The pH of HNO donation is modulated by ring substituents in Piloty's acid derivatives: azanone donors at biological pH☆

Kiran Sirsalmath, Sebastián A. Suárez, Damián E. Bikiel, Fabio Doctorovich *

Departamento de Química Inorgánica, Analítica y Química Física/INQUIMAE-CONICET, Facultad de Ciencias Exactas y Naturales, Universidad de Buenos Aires, Ciudad Universitaria, Pabellón II, Buenos Aires (C1428EHA), Argentina

ARTICLE INFO

Article history:
Received 8 June 2012
Received in revised form 10 October 2012
Accepted 10 October 2012
Available online 17 October 2012

Keywords:
Ring substituents
Piloty's acid
Azanone donors
Nitroxyl donors

ABSTRACT

A group of Piloty's acid (*N*-hydroxybenzenesulfonamide) derivatives were synthesized and fully characterized in order to assess the rates and pH of HNO (azanone, nitroxyl) donation in aqueous media. The derivatives, with electron-withdrawing and -donating substituents include methyl, nitro, fluoro, tri-isopropyl, trifluoromethyl and methoxy groups. The most interesting modulation observed is the change in pH range in which the compounds are able to donate HNO. UV–visible kinetic measurements at different pH values were used to evaluate the decomposition rate of the donors. A novel technique based on electrochemical measurements using a Co-porphyrin sensor was used to assess the release of HNO as a function of pH, by direct measurement of [HNO]. The results were contrasted with DFT calculations in order to understand the electronic effects exerted by the ring substituents, which drastically modify the pH range of donation. For example, while Piloty's acid donates HNO from pH 9.3, the corresponding fluoro derivative starts donating at pH 4.0.

1. Introduction

Azanone (nitroxyl, HNO), the one-electron reduction product of nitric oxide, is a short-lived molecule that has been intensively investigated due to its singular chemical and biological properties [1–3]. From a physiological perspective, encouraging studies suggest that azanone can be produced under particular cofactors conditions by NO-producing proteins, such as the nitric oxide synthases (NOS) [4–6]. Furthermore, several studies have shown distinct pharmacological effects for nitric oxide and nitroxyl donors, indicating that the lifetime of HNO in living tissues is probably much longer than previously assumed. This fact suggests the coexistence of HNO and NO in certain tissues [7–9]. The reactivity of nitroxyl points to hemeproteins and thiols as the biologically relevant targets [10,11].

Azanone can be generated in solution by trioxodinitrate [12] ($Na_2N_2O_3$, Angeli's salt, AS), which readily decomposes to form HNO via oxyhyponitrite anion $HN_2O_3^-$. [8] In recent years, donors that release HNO photochemically [13], thermally [14], enzymatically [15], hydrolytically [16], or by oxidation [17] have been developed. Another HNO donor is *N*-hydroxybenzenesulfonamide ($C_6H_5SO_2NHOH$, Piloty's acid, PA), which decomposes above pH 9 producing HNO through a base-catalyzed deprotonation mechanism, or releases NO upon oxidation [2,18–21].

Methanesulfohydroxamic acid (MHSA), the simplest member of the aliphatic sulfohydroxamic acid series, is also able to decompose to HNO at a rate comparable to Angeli's salt and PA [22–24]. A review addressing all the previous issues has been recently published [25].

Preparation of PA was first reported in 1896 [26]. It was firstly postulated by Angeli [27] that its decomposition occurs via elimination of azanone from the conjugate anion (Eq. (1)), analogous to the self-decomposition of AS. This is one of several examples in the literature of organic chemistry in which HNO elimination is strongly indicated.

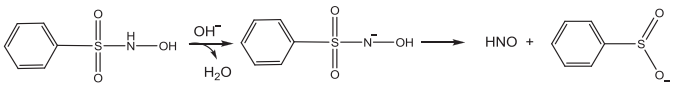

(1)

Our attention has been drawn to *N*-hydroxybenzenesulfonamide decomposition as a source of the intermediate molecule HNO, in continuation of earlier studies of this reactive species [28]. It was demonstrated by mass spectrometry that HNO is evolved during pyrolysis of the sodium salt $C_6H_5SO_2NHONa$ [29]. Exner and Juska [30] have interpreted the infrared and ultraviolet spectra of benzohydroxamic acid ($C_6H_5CONHOH$) and its alkyl derivatives under acidic, neutral, and alkaline conditions, showing their dissociable hydrogen atoms to be nitrogen bound. Infrared spectra of these and other compounds and their lithium salts in the crystalline state and in dioxane and chloroform solutions have apparently affirmed this conclusion and extended it to include PA [31]. Further evidence for N-deprotonation has been found by solid-state X-ray photoelectron spectroscopy [32]. The dissociation equilibrium thus inferred (Eq. (2)) the possibility that the intermediate species released in the decomposition

☆ Dedicated to Professor Francis T. Bonner.

* Corresponding author.
E-mail address: doctorovich@qi.fcen.uba.ar (F. Doctorovich).

0162-0134/$ – see front matter © 2012 Elsevier Inc. All rights reserved.
http://dx.doi.org/10.1016/j.jinorgbio.2012.10.008

reaction (Eq. (1)) could be the triplet molecule NOH rather than the singlet HNO.

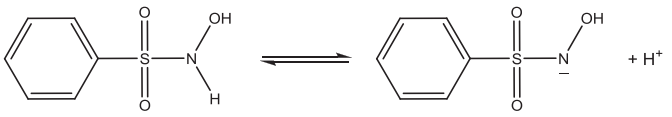

(2)

This molecule would yield triplet NO^- upon deprotonation, constituting a second example of the triplet intermediate observed in the NO–NH_2OH reaction [33,34]. Bonner and Ko [21] reported kinetic, isotopic, and NMR studies on these questions.

In this work we have studied six PA derivatives with electron-donating and -withdrawing substituents on the aromatic ring (Fig. 1 and Table 1). They have been characterized structurally and by density functional theory (DFT) calculations. Their decomposition and HNO donation capabilities have been studied as a function of pH. The substituents on the aromatic ring change the electronic properties and acidity of the $–SO_2NHOH$ group, and the N–O bond strength, allowing their decomposition (and HNO donation) to start at a large range of pH values (−1 to 10), depending on the substituents. Surprisingly enough, five of six of these donors operate at physiological pH, as it will be shown below.

2. Materials and methods

All reactions were carried out in anaerobic conditions using standard Schlenk techniques with nitrogen or argon of high purity. Manganese(III) meso-(tetrakis(4-sulfonato-phenyl)) porphyrinate (Mn^{III}TPPS) was purchased from Frontier Scientific. Hydroxylamine hydrochloride and sulfonyl chloride derivatives were purchased from Sigma-Aldrich Argentina. Magnesium oxide was purchased from Biopack. THF and methanol were purchased from Aldrich. All reagents were used without further purification. MilliQ water was employed in the kinetic experiments. Although solutions of Piloty's acid display substantial stability at low pH, they are subject to air oxidation under neutral and alkaline conditions. Hence, the solutions for the kinetic experiments were prepared fresh under anaerobic conditions and kept refrigerated until usage.

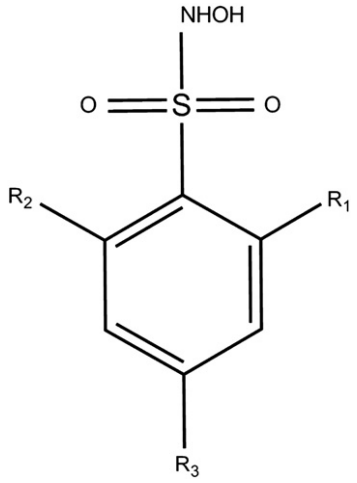

Fig. 1. Piloty's acid derivatives studied in this work. See Table 1 for R_1, R_2 and R_3.

Table 1
Names, abbreviations and substituents for the PA derivatives used in this work.

	Benzenesulfonamide	Abbreviation	R_1	R_2	R_3
1	*N*-hydroxy-4-methyl	Me-PA (or TSHA)	H	H	Me
2	*N*-hydroxy-4-nitro	NO_2-PA	H	H	NO_2
3	*N*-hydroxy-4-Fluoro	F-PA	H	H	F
4	*N*-hydroxy-2,4,6-triisopropyl	TriIso-PA	IsoP	IsoP	IsoP
5	*N*-hydroxy-4-methoxy	OMe-PA	H	H	OMe
6	*N*-hydroxy-2-nitro-4-trifluoromethyl	(NO_2–CF_3)-PA	H	NO_2	CF_3

2.1. Synthesis

N-hydroxy-4-methyl benzenesulfonamide (**1**) [35], *N*-hydroxy-4-nitro benzene sulfonamide (**2**) [35], *N*-hydroxy-4-fluoro benzene-sulfonamide (**3**) [36], *N*-hydroxy-2,4,6-triisopropyl benzene-sulfonamide (**4**) [35], *N*-hydroxy-4-methoxy benzenesulfonamide (**5**) [36], and *N*-hydroxy-2-nitro-4-trifluoro methyl-benzenesulfonamide (**6**) [24], were synthesized according to the procedure published by Porcheddu et al. [35]. NMR and other relevant analysis are reported only for the compounds which were poorly described (**5**) or not described before (**6**).

N-hydroxy-4-methoxy benzenesulfonamide (**5**). 69% yield–98% purity, mp 160 °C (dec). ^{1}H NMR (MeOD 500 MHz) 7.7 (m, 2 H), 6.9 (m, 2 H), 3.85 (s, 3 H). ^{13}C NMR (MeOD 500 MHz) 129.4 (1C), 126.7 (2 C), 112.9 (2 C), 54 (1 C).

N-hydroxy-2-nitro-4-trifluoromethyl-benzenesulfonamide (**6**). This product was prepared according to the literature procedure [35], but the reaction time was shortened to 1–2 h in order to minimize the product decomposition. It was isolated as a white solid (yield ca. 70%); mp 212–213 °C (dec.). ^{1}H NMR (DMSO, ppm): 7.51 (br s, 2H), 6.92 (s, 2 H), 4.53 (m, 2H), 2.75 (m, 1H), 1.13 (d, J = 6.9 Hz, 6H), 1.07 (d, J = 6.8 Hz, 12H). ^{13}C NMR (DMSO, ppm): 147.4, 146.9, 141.8, 121.5, 33.4, 28.2, 24.9, 23.9. Microanalysis did not fit the calculated values due to the fast spontaneous decomposition of the product.

2.2. Instrumental procedures

All known compounds were characterized by melting point, ^{1}H, and ^{13}C NMR. The analysis agreed with the previously reported ones [35–37]. The amount of solvent present in the molecular formula was determined by ^{1}H NMR spectra and microanalysis. Melting points were taken on a capillary melting point apparatus. ^{1}H NMR and ^{13}C NMR spectra were measured in $CDCl_3$ on a Bruker AM 500 spectrometer using tetramethylsilane as internal standard.

2.3. Kinetic measurements

Spontaneous decomposition of the donors was followed at various pH values. Kinetic data were obtained measuring the UV absorbance spectra change in a HP 8453 spectrometer using a 1-cm path quartz cell sealed with a septum ensuring an inert atmosphere. The temperature was controlled using a Lauda RE 207 thermostat at 25 °C. All the solutions were degassed for 20 min before the experiment using N_2 or Ar. The pH was controlled by proper buffer solutions (ca. 0.1 M). Reactions were unaffected by the irradiation of the sample with the light source of the spectrometer. Donor solutions were freshly prepared for each set of measurements and kept on ice and the concentration was checked before each measurement by UV–vis following its absorbance. Donors were dissolved in ethanol 96%, and added to the porphyrin solutions to a final ethanol/water ratio smaller than 1%. The kinetic data were analyzed by a program written in MATLAB2008a, which allows fitting the experimental data to a particular proposed mechanism. It is composed by a singular value decomposition (SVD) subroutine which extracts the

relevant data, diminishing the noise and a minimization subroutine which uses the simplex algorithm of Nelder–Mean to adjust the proposed kinetic constants. In addition to the decomposition UV–visible experiments, kinetic experiments were conducted by ^{1}H NMR in an AM500 Bruker spectrometer. In all cases only one organic product was observed by NMR, identified as the corresponding sulfinate by comparison with the reported infrared spectra (see Supplementary Information (SI)) [38].

2.4. Measurements of HNO production as a function of pH

In all cases the current intensity, which corresponds to the electrical response to HNO generated by decomposition of the donors, was measured with the electrode described in previous literature [39]. Under inert atmosphere, 0.015 mmol of donor were added to 15 mL of an 0.1 M KNO_3 aqueous solution at the initial pH, which was previously adjusted by addition of HCl (aq.) (initial pH = 2 for all donors). The pH was raised slowly by addition of 0.01 M aqueous NaOH up to pH = 11. Current intensity, time and pH were recorded simultaneously with the setup shown in Figure SI1.

2.5. Single-crystal diffraction studies

All crystal donors were obtained by slow diffusion from acetonitrile at room temperature and were mounted on a nylon loop. Single-crystal data were collected on an Oxford Diffraction Gemini E CCD Diffractometer equipped with a sealed tube with Mo KR radiation (λ = 0.71073 Å) at room temperature. For data collection, cell refinement and data reduction CrysAlis PRO software was used. Absorption correction was made by multi-scan. The structures were solved using direct methods with SHELXS-97 and refined by the full-matrix least-squares technique with SHELXS-97 based on F2. Software used to prepare material for publication: WinGX publication routines and ORTEP-3 for Windows. See Table SI1 for experimental data.

2.6. DFT calculations

All gas-phase DFT calculations performed in this work were carried out using the Gaussian 98 software package. Calculations were carried out at two different levels of theory. Geometries were fully optimized at the B3P86 level using 6–311 + G(2df,p) for all atoms in order to obtain comparable geometrical parameters against DRX bonds. Optimizations at the B3LYP level using 6–31 G(d,p) for all atoms using water (polarizable continuum model—PCM) were used in order to take into account solvation effects of the energetics of the reactions. Deprotonation reactions were modeled using an explicit water molecule as the proton acceptor. The NOH molecule was calculated in the triplet state, while all the remaining molecules were calculated as singlets.

3. Results and discussion

The selected PA derivatives contain electron attracting (**2**, **3**, **6**) and donating groups (**1**, **4**,**5**). In the case of **4** there is also an important steric hindrance around the $–SO_2–NHOH$ moiety. All donors were prepared by following a recently described method (Eq. (3)) [35]. Since some of these derivatives were not reported with this synthetic procedure, Table 2 shows the yields obtained for all derivatives, which are very good. Unfortunately, the derivative **6** decomposes spontaneously in the course of a few hours even in the solid form.

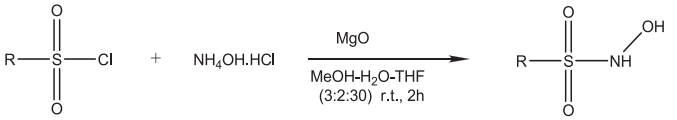

(3)

Table 2
Isolated yields of PA derivatives used in this work.

Product	R	Yield (%)
1	4-MeC_6H_4	85
2	4-$O_2NC_6H_4$	97
3	4-FC_6H_4	96
4	2,4,6-$(i\text{-}Pr)_3C_6H_2$	90
5	4-$OMeC_6H_4$	72
6	2-NO_2-4-$CF_3C_6H_4$	ca 70

In order to obtain the effect of the pH of the medium over the decomposition of the compounds, we ran UV–vis kinetics at different pH values for each compound, at 25 ° C (see Fig. S1). The decomposition rates were tested at various pH values in independent experiments, and the approximate pH at which the decomposition started to be observed was determined (as asserted by following the UV–vis and/or the ^{1}H NMR spectra for 5 h). Table 3 shows the rate constants for the decomposition of the PA derivatives, which was modeled as a first order reaction. As can be observed in Table 3, the decomposition rate is in all cases in the range 10^{-3} to 10^{-4} s^{-1}. However, the pH at which the donors start to decompose shows a broad range (ca. 10 pH units). This cannot be due to a change in acidity of the –NHOH substituent only, since for example in the case of arenesulfonic acids similar substituents on the aromatic ring produce a change on the acidity of the $–SO_3H$ group of less than 1 pH unit (−7.18 for *p*-NO_2 versus −6.57 for *p*-CH_3) [40]. On the other hand, OMe-PA, containing en electron-donor substituent, decomposes at the same pH than NO_2-PA, which contains an electron-attracting substituent. Therefore, other factors such as the N–O bond strength of the $–SO_2–NHOH$ moiety and solvation effects should be considered, as it will be discussed below.

The pH at which the donation of HNO starts was determined in each case by using an HNO-selective electrode [39], which signal comprises a current proportional to [HNO] and is completely insensitive to NO. Starting with a solution of the donor at a pH in which the compound is stable, the pH was raised slowly by addition of diluted NaOH(aq.), while the pH and current were measured simultaneously. A large increase in the current indicates that [HNO] is raising, reaching a plateau when the maximum rate of HNO formation is obtained. Table 3 shows that the inflexion point of the current vs. pH curve is in most cases around one pH unit after the pH at which the decomposition starts to be observed, except for TriIso-PA (Fig. 2, the rest of the curves are shown in Fig. SI2).

In some cases suitable crystals for X-ray diffraction experiments could be obtained. The structures are shown in Fig. 3 and relevant parameters are listed in Table 4. The S–N bond distances are quite

Table 3
Rate constants for the decomposition of Piloty's acid derivatives.

	Product	Rate constant (k, s^{-1})[a]	Decomposition pH[b]	HNO donation pH[c]
	PA	$(2.44 \pm 0.23) \times 10^{-4}$ [21]	9.3 [21]	–
1	Me-PA	$(4.4 \pm 0.6) \times 10^{-4}$	9	10.0 ± 0.5
2	NO2-PA	$(3.6 \pm 0.4) \times 10^{-4}$	5	5.7 ± 0.8
3	F-PA	$(1.9 \pm 0.3) \times 10^{-3}$	3	4.0 ± 0.3
4	TriIso-PA	$(5.0 \pm 0.5) \times 10^{-3}$	3	5.4 ± 0.2
5	OMe-PA	$(3.5 \pm 0.4) \times 10^{-4}$	5	5.8 ± 0.7
6	(NO_2-CF_3)-PA	$(6.3 \pm 0.8) \times 10^{-4}$	ca. −1	Not measured

[a] Rate constant at the pH where the HNO electrode current reaches a plateau (Figs. 2 and SI2). In the case of **6**, the rate was taken two pH units after the decomposition pH.
[b] pH at which decomposition starts to be observed by UV–visible and/or NMR.
[c] Inflexion point for the current vs. pH curves (Figs. 2 and SI2).

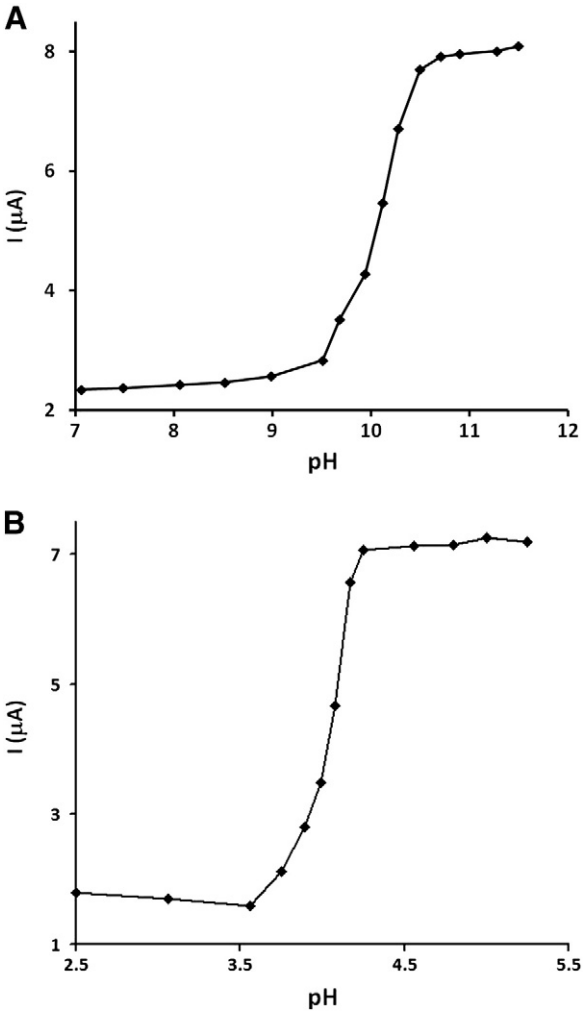

Fig. 2. pH versus HNO current intensity for: a) Me–PA b) F–PA.

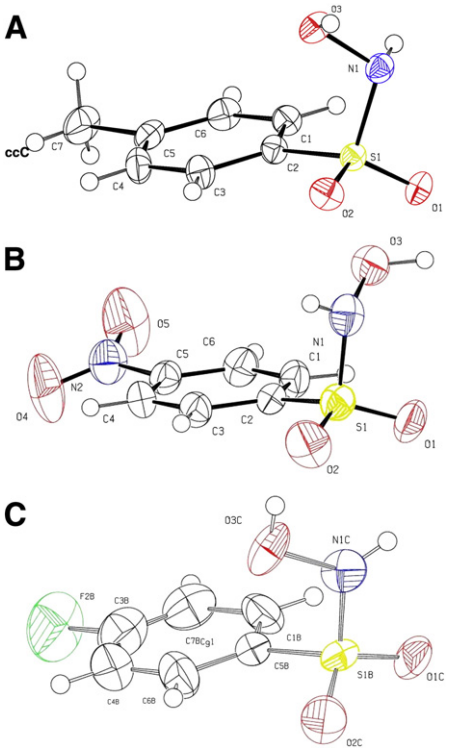

Fig. 3. Crystal structure of: a) Me–PA; b) NO_2–PA; c) F-PA. Ellipsoids are drawn at 50% probability level.

similar in all cases. However, the N–O bond tends to be shorter when electron-attracting groups are present in the ring (–NO_2, –F). This shorter bond would facilitate the formation of HN = O, which requires a double bond between the N and O atoms. The trend shown in Table 4 is quite in agreement with the HNO donation pH values listed in Table 3. However, it has to be taken into account that the situation predominating in solution could differ from solid-state measurements.

3.1. NH versus OH deprotonation, and electron-withdrawing versus electron-donating groups

Deprotonation as the first step for PA decomposition has been suggested initially by Angeli [27]. The –SO_2NHOH moiety contains two proton-like hydrogen atoms, one on the N atom and the other one on the O atom. One question that arises is which proton loss (from O–H or N–H) is more relevant for the decomposition pathway. By means of electronic structure calculations we optimized the structures for TSHA (Me-PA), its two derived monoanions, and the dianion. The deprotonation processes are depicted in Scheme 1. The results show that both deprotonations hold similar energetic requirements, with N-deprotonation producing a more stable anion than O-deprotonation by ca. 10 kcal/mol. However, decomposition from the O-anion is more favorable than from the N-anion by almost 30 kcal/mol. Moreover, O-deprotonation to form the corresponding anion sets the –SO_2NHOH moiety to release HNO while in the case of the N-anion, the breakage of the S–N bond produces the NOH isomer which eventually can convert to HNO. The process ^{3}NOH → ^{1}HNO is favorable from the energetic point of view, −15.5 kcal/mol according to our calculations, ca. −20 kcal/mol by measurements from previous lit. [41], but it has to be taken into account that this triplet to singlet process is forbidden and could be relatively slow. Summarizing, taking into account the energetic requirements, in aqueous media O-deprotonation and the subsequent ^{1}HNO release seems more likely to take place than N-deprotonation and ^{3}NOH release, contrary to what have been suggested before in organic solvents. [31] Regarding the second deprotonation, the energy release from the N-anion to yield the dianion is the highest one. From this point, the breakage to produce NO^- is a very favorable process, suggesting that at extremely high pH values, NO^- could be formed directly from the dianion.

For the rest of the PA derivatives, all energies discussed above were also calculated (SI and Table 5). Table 5 presents the calculated energies for the processes:

$$\mathrm{O-deprotonation}(\Delta E_{\mathrm{OH}}) \quad (4)$$
$$\mathrm{R-SO_2{-}NH{-}OH \rightarrow [R-SO_2{-}NH{-}O]^- + H^+}$$

$$\mathrm{N-deprotonation}(\Delta E_{\mathrm{NH}}) \quad (5)$$
$$\mathrm{R-SO_2{-}NH{-}OH \rightarrow [R-SO_2{-}N{-}OH]^- + H^+}$$

$$\mathrm{Decomposition\ from\ O-anion}(\Delta E_{\mathrm{HNO}}) \quad (6)$$
$$\mathrm{[R-SO_2{-}NH{-}O]^- \rightarrow [R-SO_2]^- + HNO + H^+}$$

$$\mathrm{Decomposition\ from\ N-anion}(\Delta E_{\mathrm{NOH}}) \quad (7)$$
$$\mathrm{[R-SO_2{-}N{-}OH]^- \rightarrow [R{-}SO_2]^- + NOH + H^+}$$

The trends presented in Table 5 can be rationalized in terms of the electron-donating/withdrawing nature of the substituent. In fact, the easiest deprotonation occurs for the nitro derivative which can be assumed to have the most positively charged –NHOH group and hence the most stable anion. On the other hand, –OMe (an electron-

Table 4
Relevant experimental bond distances and angles.

Compound	d_{S-N} (Å)	d_{N-O} (Å)	<SNO (°)
Me-PA	1.659	1.431	110.34
PA	1.645	1.414	109.67
NO2-PA	1.656	1.407	111.16
F-PA	1.649	1.392	108.56

donating group at the *para* position, but electron-withdrawing by inductive effect at the *meta* position) destabilizes the anion formed at the *para* position and hence its deprotonation is less favorable. The effects are more important for the electron-withdrawing than for the donating groups. For example, for the deprotonation of –OH the difference between PA ("H" substituent) and the strongest electron-withdrawing nitro group (**2**) amounts 3.6 kcal/mol, while the difference with the electron-donating methoxy group (**5**) is only of 0.9 kcal/mol. This last difference is reduced if a water molecule H-bound to the –OMe group is added to the calculations (see Table 5 and Fig SI4), and in the presence of two water molecules it is reduced even further. This tendency and the previously shown experimental evidence indicate that in aqueous solution the electron-attracting inductive effect of the *para* –OMe group predominates over the electron-donating resonance effect. In the same direction, if we analyze the relative stability of the sulfinate anions produced (Figure SI5 and Table SI4), while the electron-withdrawing substituents generate more stable anions, electron donor ones produces the opposite effect. In fact, there is a clear trend between the relative energy of the sulfinate anion and the energy of the HNO donation process. TriIso-PA is an exception, since it is more prone to donate HNO than the sulfinate stability suggests, probably due to steric constraints (i.e. longer S–N bond).

All these trends can be also rationalized by using a free-energy correlation function such as the Hammett equation. Fig. SI3 shows a plot of the σ_p Hammet parameters versus the OH and NH deprotonation energies ΔE_{OH} and ΔE_{NH}. The correlation is not far from linearity and in agreement with the previous comments.

The acidity corresponding to the NH and OH groups can be estimated by using $\Delta G° = -RTlnK$, assuming that the fundamental differences between the different compounds are due to the enthalpic contribution. Given two different donors:

$$\Delta G_2 - \Delta G_1 = -RTlnK_2 + RTlnK_1 \quad (8)$$

Table 5
Calculated energies for reactions 1–4 (kcal/mol), and estimated pK_a values for compounds **1** to **5**.

	R	ΔE_{OH}	ΔE_{NH}	$pK_{a(NH)}$	ΔE_{HNO}	ΔE_{NOH}
	H	56.1	44.4	9.29 [21]	−1.0	26.2
1	Me	56.6	45.1	9.8	−0.6	26.5
2	NO_2	52.5	40.0	6.0	−3.2	24.8
3	F	55.5	43.9	8.9	−1.3	25.9
4	iPr_3	55.0	45.7	10.3	−3.8	21.1
5	OMe	57.0	45.7	10.3	−0.3	26.6
		(56.7)[a]	(45.3)[a]		(−0.5)[a]	(26.4)[a]

[a] Calculated with the addition of one water molecule H-bound to **5**.

which can be rearranged to yield:

$$K_2 = K_1 exp(-(\Delta G_2 - \Delta G_1)/RT) \quad (9)$$

and according to the proposed approximation

$$K_2 = K_1 exp(-(\Delta E_2 - \Delta E_1)/RT) \quad (10)$$

By using one of the compounds as standard (i.e. PA with $pK_a = 9.29$), the remaining pK_a values can be calculated. The pK_a values corresponding to ΔE_{NH} are shown in Table 5, and similar results are obtained if the pK_a values corresponding to ΔE_{OH} are calculated. As it can be observed there is a good agreement between the calculated pK_a and the HNO donation pH (Table 3) in the cases of **1** and **2** ($pK_{a(NH)} = 9.8$ and 6.0 vs. HNO donation pH = 10.0 and 5.7 respectively). However, the HNO donation pH values of **3**, **4** and **5** are ca. 5 pH units smaller than the estimated pK_a values.

4. Conclusions

Piloty's acid derivatives have been synthesized and the pH values at which HNO donation starts were determined by measurement of the released HNO. These values are approximately coincident with the pH values of decomposition, which cover a broad pH range (ca. −1 to 10).

From the kinetic point of view, the stability of the anions derived from the donors is similar, since the decomposition rate constants are all in the range 10^{-3}–10^{-4}. However, F-PA and TriIso-PA, show the fastest decomposition rates, and therefore a kinetic effect could be predominating in these cases. In the case of PA, as well as for the donors

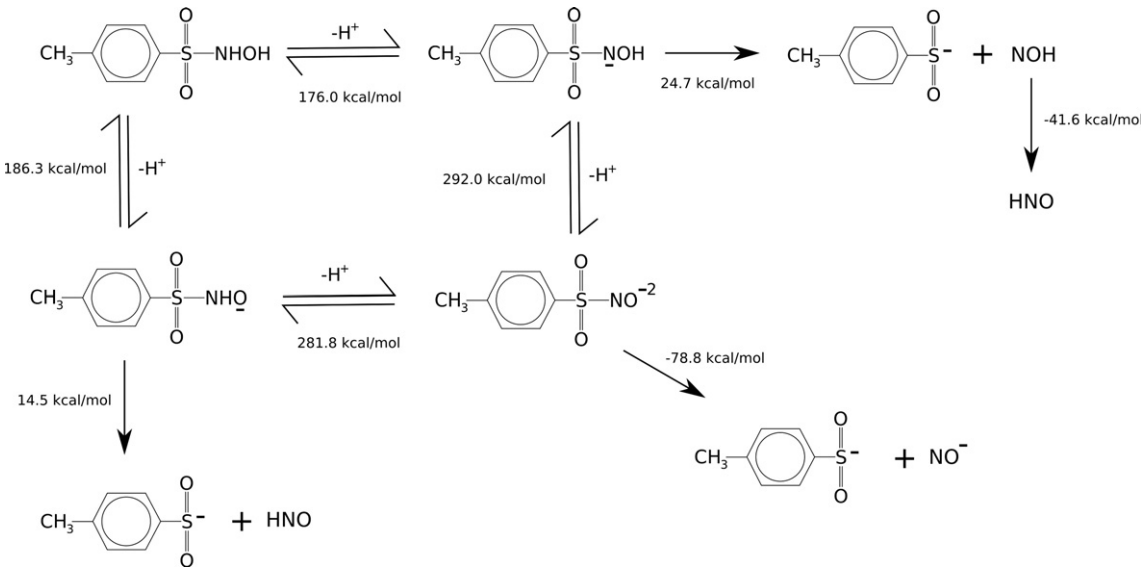

Scheme 1. Mechanisms of HNO/NO– donation from TSHA.

NO_2-PA and Me-PA, the pH at which the HNO donation starts seems to be dominated by the thermodynamic acidity constants. However, another predominant effect seems to be "structural." Table 4 shows a clear tendency; d_{N-O} is in the order: F-PA (**3**)<NO_2-PA(**2**)<PA<Me-PA (**1**) which follows the same trend than the HNO donation pH. This could be due to the fact that the shorter this bond is, more facile results the formation of HN=O. One would expect to see this situation reflected in the ΔE_{HNO} values of Table 5, which are more favorable for NO_2-PA, F-PA and TriIso-PA. However, these differences are rather small and the solvent could be playing an important role enhancing these variations through H-bonding to the N and O atoms of the HNO moiety. Finally, steric hindrance may be important in the case of TriIso-PA, and solvation is definitely expected to be important in the case of OMe-PA through H-bonding to the –OMe group.

Contrary to PA and TSHA, the rest of the donors with electron-attracting or withdrawing substituents work as HNO donors at physiological pH. All these PA derivatives are easily synthesized in one-step reactions from the corresponding sulfonyl chlorides with very good to excellent yields. Since a large variety of sulfonyl chlorides is commercially available, an enormous number of donors derived from PA working at any pH are available one step away.

Abbreviations

AS	trioxodinitrate—$Na_2N_2O_3$—Angeli's salt
PA	*N*-hydroxybenzenesulfonamide—Piloty's acid
Me-PA (or TSHA)	*N*-hydroxy-4-methylbenzenesulfonamide
NO_2-PA	*N*-hydroxy-4-nitro benzenesulfonamide
F-PA	*N*-hydroxy-4-fluorobenzenesulfonamide
TriIso-PA	*N*-hydroxy-2,4,6-triisopropylbenzenesulfonamide
OMe-PA	*N*-hydroxy-4-methoxybenzenesulfonamide
(NO_2–CF_3)-PA	*N*-hydroxy-2-nitro-4-trifluoromethyl benzenesulfonamide
Mn^{III}TPPS	manganese(III) meso-(tetrakis(4-sulfonato-phenyl)) porphyrinate
DFT	density functional theory
PCM	Polarizable Continuum Model

Acknowledgements

This work was financially supported by UBA (UBACYT W583), FONCyT (PICT 2010-2649), CONICET (PIP 112-201001-00125) and PME-2006-01113.

Appendix A. Supplementary data

Supplementary data to this article can be found online at http://dx.doi.org/10.1016/j.jinorgbio.2012.10.008.

References

[1] P.J. Farmer, F. Sulc, J. Inorg. Biochem. 99 (2005) 166–184.
[2] K.M. Miranda, Coord. Chem. Rev. 249 (2005) 433–455.
[3] C.H. Switzer, W. Flores-Santana, D. Mancardi, S. Donzelli, D. Basudhar, L.a. Ridnour, K.M. Miranda, J.M. Fukuto, N. Paolocci, D.a. Wink, Biochim. Biophys. Acta 1787 (2009) 835–840.
[4] S. Adak, Q. Wang, D.J. Stuehr, J. Biol. Chem. 275 (2000) 33554–33561.
[5] A.J. Hobbs, J.M. Fukuto, L.J. Ignarro, Proc. Natl. Acad. Sci. 91 (1994) 10992–10996.
[6] H.H.H.W. Schmidt, H. Hofmann, U. Schindler, Z.S. Shutenko, D.D. Cunningham, M. Feelisch, Proc. Natl. Acad. Sci. 93 (1996) 14492–14497.
[7] K.M. Miranda, N. Paolocci, T. Katori, D.D. Thomas, E. Ford, M.D. Bartberger, M.G. Espey, D. a Kass, M. Feelisch, J.M. Fukuto, D.A. Wink, Proc. Natl. Acad. Sci. 100 (2003) 9196–9201.
[8] D.A. Wink, K.M. Miranda, T. Katori, D. Mancardi, D.D. Thomas, L. Ridnour, M.G. Espey, M. Feelisch, C.A. Colton, J.M. Fukuto, P. Pagliaro, D.A. Kass, N. Paolocci, Am. J. Phys. 285 (2003) H2264–H2276.
[9] P. Pagliaro, Life Sci. 73 (2003) 2137–2149.
[10] M.P. Doyle, S.N. Mahapatro, R.D. Broene, J.K. Guy, J. Am. Chem. Soc. 110 (1988) 593–599.
[11] K.M. Miranda, R.W. Nims, D.D. Thomas, M.G. Espey, D. Citrin, M.D. Bartberger, N. Paolocci, J.M. Fukuto, M. Feelisch, D.A. Wink, J. Inorg. Biochem. 93 (2003) 52–60.
[12] D.A. Wink, M. Feelisch, J. Fukuto, D. Chistodoulou, D. Jourd'heuil, M.B. Grisham, Y. Vodovotz, J.A. Cook, M. Krishna, W.G. DeGraff, S. Kim, J. Gamson, J.B. Mitchell, Arch. Biochem. Biophys. 351 (1998) 66–74.
[13] K. Matsuo, H. Nakagawa, Y. Adachi, E. Kameda, H. Tsumoto, T. Suzuki, N. Miyata, Chem. Commun. (Camb. UK) 46 (2010) 3788–3790.
[14] D.A. Guthrie, N.Y. Kim, M.A. Siegler, C.D. Moore, J.P. Toscano, J. Am. Chem. Soc. 134 (2012) 1962–1965.
[15] H.T. Nagasawa, E.G. DeMaster, B. Redfern, F.N. Shirota, D.J.W. Goon, J. Med. Chem. 33 (1990) 3120–3122.
[16] X. Sha, T.S. Isbell, R.P. Patel, C.S. Day, S.B. King, J. Am. Chem. Soc. 128 (2006) 9687–9692.
[17] B.-B. Zeng, J. Huang, M.W. Wright, S.B. King, Bioorg. Med. Chem. Lett. 14 (2004) 5565–5568.
[18] M.J. Lee, D.W. Shoeman, D.J. Goon, H.T. Nagasawa, Nitric Oxide 5 (2001) 278–287.
[19] R. Zamora, A. Grzesiok, H. Weber, Biochem. J. 339 (1995) 333–339.
[20] P.C. Wilkins, H.K. Jacobs, M.D. Johnson, A.S. Gopalan, Inorg. Chem. 43 (2004) 7877–7881.
[21] F.T. Bonner, Y. Ko, Inorg. Chem. 31 (1992) 2514–2519.
[22] D.W. Shoeman, H.T. Nagasawa, Nitric Oxide 2 (1998) 66–72.
[23] F.N. Shirota, E.G. DeMaster, M.J. Lee, H.T. Nagasawa, Nitric Oxide 3 (1999) 445–453.
[24] J.P. Toscano, F.A. Brookfield, L.M. Cohen, Andrew D. Courtney, Stephen Martin Frost, V.J. Kalish, WO 2007/109175 A1.
[25] F. Doctorovich, D. Bikiel, J. Pellegrino, S.A. Suárez, A. Larsen, M.A. Martí, Coord. Chem. Rev. 255 (2011) 2764–2784.
[26] O. Piloty, Ber. Dtsch. Ges. 29 (1896) 1559.
[27] A. Angeli, Chem. Zentralbl. 73 (1902) 691.
[28] F.T. Bonner, M.N. Hughes, Comments Inorg. Chem. 7 (1988) 215–234.
[29] F. Seel, C. Bliefert, Z. Anorg. Allg. Chem. 406 (1974) 277–281.
[30] O. Exner, T. Juska, Collect. Czech. Chem. Commun. 49 (1984) 51.
[31] O. Exner, Collect. Czech. Chem. Commun. 29 (1964) 1337.
[32] O. Exner, B. Kalkac, Collect. Czech. Chem. Commun. 28 (1963) 1656.
[33] F.T. Bonner, N.Y. Wang, Inorg. Chem. 25 (1986) 1858–1862.
[34] N.Y. Wang, F.T. Bonner, Inorg. Chem. 25 (1986) 1863–1866.
[35] A. Porcheddu, L. De Luca, G. Giacomelli, Synlett (2009) 2149–2153.
[36] G.M. Blackburn, B.E. Mann, B.F. Taylor, A.F. Worrall, Eur. J. Biochem. 153 (1985) 553–558.
[37] J.N. Scholz, P.S. Engel, C. Glidewell, K.H. Whitmire, Tetrahedron 45 (1989) 7695–7708.
[38] B.J. Lindberg, Acta Chem. Scand. 21 (1967) 2215–2234.
[39] S.A. Suárez, M.H. Fonticelli, A.A. Rubert, E. de La Llave, D. Scherlis, R.C. Salvarezza, M.A. Martí, F. Doctorovich, Inorg. Chem. 49 (2010) 6955–6966.
[40] D.C. French, D.S. Crumrine, J. Org. Chem. 55 (1990) 5494–5496.
[41] A. Luna, M. Merch, B. Srn, O. Roos, Chem. Phys. 196 (1995) 437–445.